Solubility Predictions for Sodium Nitrate from Water Activity for Hanford Tank Concentrates – 15551

Stephen Agnew *, Gene Ramsey **
* Columbia Energy & Environmental Services, Inc.
** Washington River Protection Solutions

ABSTRACT

Space in Hanford waste tanks is very limited and therefore active evaporation of tank liquids continues to provide a means to conserve tank space. Prior to each evaporator campaign, a boildown of a sample of tank liquid provides a basis for planning by measuring density, solids precipitation, and water activity as a function of concentration and temperature. We have found these datasets also provide opportunities to validate and calibrate various solubility models on actual waste.

Previous work has shown the solubilities of minor electrolytes in these five boildowns follow rather simple power law solubility products. Each of five boildowns concentrated liquids from five waste tanks and tank blends and have been reported from Hanford's 222-S laboratory. All concentrates eventually showed the precipitation of the dominant electrolyte, $NaNO_3$, and solution activity largely drives this solubility. Although there are many well established techniques for calculating solution activity, the complexity of Hanford electrolyte mixtures has proven challenging for such solution activities.

Accurate predictions of water activity for these concentrates provides an alternative method for calculating solution activity and previous work has validated a relatively simply model for predicting the water activity of even complex electrolyte mixtures. Given such a water activity, a Gibbs-Duhem integration of that water activity accurately predicts the solution activity and therefore the solubility of $NaNO_3$ at 18°C with a correlation coefficient of 0.94 over a wide range of liquid waste compositions for these boildown studies.

To our knowledge, no other solubility prediction has correlated as highly with measured solubility points of $NaNO_3$ in any complex electrolyte mixture. Better predictions of $NaNO_3$ solubility in complex waste mixtures improve planning for recovery of waste tank space and reduce the need for new tank space.

INTRODUCTION

The recovery of tank space by means of active evaporation of waste liquids has been a very common function at Hanford for over fifty years. While in the past only minimal studies were performed on tank liquids prior to concentration, much more detailed boil-down studies [1-5] precede each recent waste reduction campaign.

This paper will show how these detailed boil-down studies are a very valuable means to calibrate solubility models for various waste species. At some point during concentration, each of the electrolytes precipitate and therefore provide a basis for validating model predictions. The phosphate-fluoride double salt, for example, was saturated even in the initial solutions. In contrast, there were no Al solids that formed during any of the boildown tests. Aluminum precipitates as the neutral $Al(OH)_3$ despite being an electrolyte in solution as aluminate, $Al(OH)_4^-$ and various solubility models predict that Al is supersaturated in many of these solutions.

We will show how after fitting a water activity model to reported water activities, a Gibbs-Duhem integration of water activity provides a thermodynamic prediction for $NaNO_3$ solubility.

METHODOLOGY

Previous reports describe [1-5] the detail of liquid samples from five different tanks and tank blends and only the salient features are described here. Samples from five different tanks and tank blends were evaporated at three constant pressures of 40, 60, and 80 torr until an excess of 20 vol% solids precipitated. The temperature varied accordingly from 40-60°C during each boildown and resulted in precipitation of various minor solids very early and eventually major electrolytes precipitated, usually $NaNO_3$ and Na_2CO_3.

An example of the major species concentrations appear in Fig. 1 and minor species in Fig. 2, both as a function of free hydroxide for AP-105. Free hydroxide is a convenient metric of the concentration since it does not result in any precipitates and is therefore proportional to volume reduction. Each boildown consisted of 6-10 assays of extracts from the bottoms during the boildown. Extracted samples were cooled to 18°C for five days and then assayed for liquid composition and solids phase identification.

Figure 1. Major species molarities for boildown of AP-105.

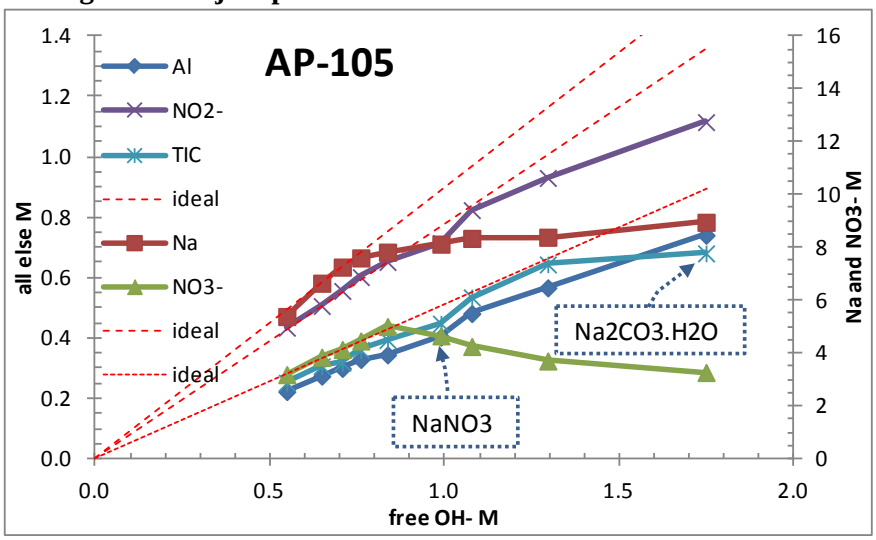

Concentration of major species versus free hydroxide for the boildown of a sample of AP-105. Species that deviate from the dashed ideal lines, i.e. simple volume concentration, have precipitated.

The ideal lines in Figs. 1 and 2 are extrapolations of the ideal concentrations for species given the volume concentration and no precipitation.

Vapor pressures were kept constant relative to absolute barometric pressure and were therefore water activities. Each boildown measured solution vapor pressure ratio with the vapor pressure of pure water at temperature given the Antoine equation of state for water [6].

Water Activity by Solvation Cluster Equilibria

Precipitated solids with waters of hydration depend on the activity of water and both phosphate and aluminate solubilities therefore depend on water activity. Aluminum solubility depends on the equilibrium between aluminate and its dimer, which in turn depends on water activity as well as on the entropy of mixing due to the complexity of the solution mixture. To estimate water activity, we used the

solvation cluster equilibria (SCE) model [7] with parameters K and n fitted to the mixtures with linear regression.

Figure 2. Concentrations of minor species for boildown of AP-105.

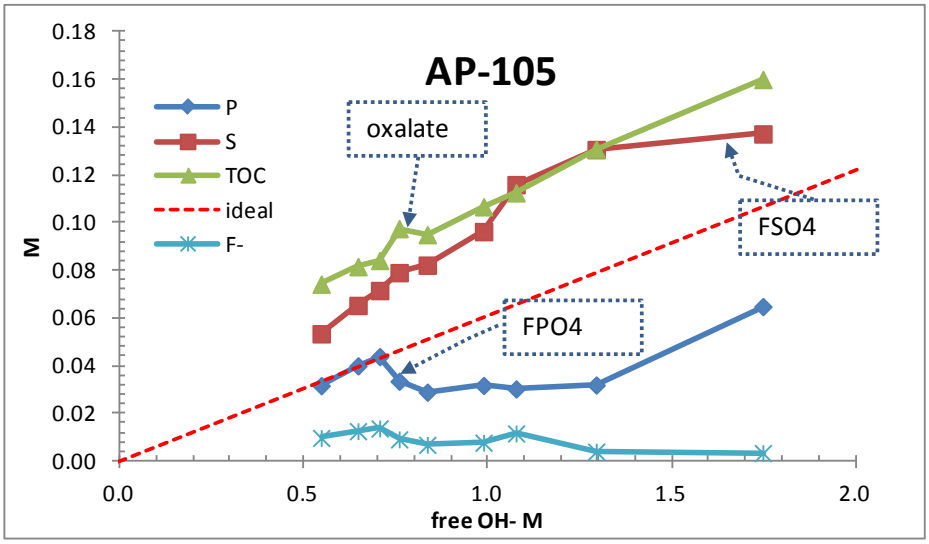

Minor species concentrations versus free hydroxide for boildown of AP-105. Deviations from the dashed ideal line, i.e. simple volume concentration, indicate precipitation of phosphate as $Na_3PO_4.(NaF.19H_2O)_{0.5}$ and $Na_2SO_4.NaF$ precipitates from its ideal line (not shown) as well. Plot shows phosphate as P and sulfate as S.

$$a_w = \frac{1}{1+\frac{m}{55.51}+\gamma_{mix}\gamma_{DH}\left(\frac{1.1723}{\left(\frac{1}{\sqrt{m}}+1\right)}\left(\frac{\sum f_i K_i}{1+\frac{55.51}{m}}\right)\right)^{\sum f_i n_i}} \qquad \text{(Eq. 1)}$$

For the Hanford tank waste liquids, we have fit K_i and n_i for each of NaOH, $NaAl(OH)_4$, $NaNO_3$, and $NaNO_2$ by least squares regression to the water activity data.

$$\gamma_{mix} = \left(1+m/55.51\right)^{1/(1+m/55.51)}\left(1/f_{iNa}+55.51/f_{iNa}m\right)^{f_{iNa}m/(m+55.51)}\prod_i\left(55.51/f_i f_{iX}m+1/f_i f_{iX}\right)^{f_i f_{iX} m/(m+55.51)}$$

$$m = \sum \nu_i m_i$$

K_i = SCE hydration equilibrium constant
n_i = SCE hydration order, m_i is molality of electrolyte i
ν_i = the SCE effective ion number for electrolyte i
f_i = fraction of electrolyte I
$\gamma_{DH} = e^{-1.1723/\left(\frac{1}{\sqrt{m}}+1\right)}$ Debye-Hückel factor (no parameters, assumed = 1 for fit)
γ_{mix} = entropy of mixing factor (no parameters)
$n = \Sigma\, f_i\, n_i$, weighted average n, hydration order

Gibbs-Duhem Integration

$$\frac{\Delta G_{sol} - \Delta G_{res} + T\Delta S_{mix}}{RT} = \ln\left(a_o \gamma_{SCE} \gamma_{DH} m\right) = 55.51 \int_{1-\varepsilon}^{x1} \frac{da_w}{m a_w} + \ln\left(a_o \gamma_{DH} m\right) \quad \text{(Eq. 2)}$$

ΔG_{sol} free energy of solvation
ΔG_{res} residual free energy of solvation; electrolyte interactions that do not impact water activity
ΔS_{mix} entropy of mixing

When an electrolyte dissolves in solution, ΔG_{sol} expresses the free energy change due to solvating the ions of that electrolyte. In principle, mixtures of electrolytes will simply additive to an overall solution activity, a_o. However, an additional entropy of mixing, ΔS_{mix}, increases the solution free energy further and there are residual free energy, ΔG_{res}, interactions among species that don't directly impact solution activity.

Residual free energy represents bonding interactions between and among ions that do not necessarily impact water activity and therefore do not show up as part of the integration. These interactions include a large number of factors and are very difficult to predict, and so there are various approaches for accounting for ΔG_{res}.

The SCE solution water activity, a_w, integrated by means of the Gibbs-Duhem relation, Eq. 2, gives the electrolyte mixture activity and free energy at as function of molality, m, without any additional adjustable parameters.

Instead of a functional form for each electrolyte activity, a_i, the SCE begins with a functional form for the electrolyte mixture water activity, a_w, based on the mol fraction weighting of each pure electrolyte's SCE parameters.

Given two parameters for each pure electrolyte, an SCE regression to the set of measured water activities provided an analytic a_w for the Gibbs-Duhem integration. The SCE's simplified analytic expression for a mixture's water activity is still empirical, and yet includes a solution free energy that then provides a means for estimating very complex mixtures.

The SCE activity function is a product of SCE ion hydration with its three parameters per electrolyte and Debye-Hückel charge compression with one parameter per mixture vector. The SCE electrolyte hydration factor represents an equilibrium among electrolyte weakly bound waters. The amount of weakly bound water is affected not only by the nature of each electrolyte but also by an mean long-range charge compression due to all electrolytes in a mixture.

Electrolyte solvation involves many short and long range static and dynamic phenomena [8]. The SCE model comprises just these four basic phenomena:

1) Colligative, the dilution of species due to atomicity;
   –ion association reduces atomicity;
2) Ion hydration, the bonding of water to ions inner and outer solvation spheres;
3) Long range electrostatic solvent compression, i.e. the Debye-Hückel factor;
4) Each mixture of electrolytes has an excess ΔG_{res} due to bonding between pairs of electrolytes that does not impact system activity;

The SCE and just these four phenomena appear to be consistent with measurements of water activity for Hanford electrolyte solutions and related electrolytes.

Ion Balance

It is important that the solution compositions show ion balance since fitting parameters to solutions with ion balance errors results in fits that reflect those errors. There are many uncertainties and systematic errors in solubility modeling and ion balance is one of the many sources of uncertainty. We have therefore balanced the ions with a simple expedient of adjusting cations and ions to their averages.

Although ion balance can be off due to either or both cation and anion measurements, we have assumed that both cation and anion measurements are equally in error. This means that cations are adjusted as

$$C_{Na} = C_{Na} * (1+ C_{anions} / C_{cations}) / 2$$

while anions are adjusted as

$$C_{NO3} = C_{measNO3} * (1+ C_{cations} / C_{anions}) / 2 \ .$$

RESULTS AND DISCUSSION

Table I shows the initial concentrations for all of the boildowns. The dominant species is nitrate and nitrate is the major precipitate observed in all cases followed by carbonate and then nitrite. However, the minor precipitates of phosphate-fluoride, oxalate, and sulfate-fluoride were also observed for all boildowns. The uncertainties for the boildown assays are discussed in each of the reports. [1-5]

Water Activity by Solvation Cluster Equilibria

Regressing the SCE parameters with two parameters for each species NaOH, $NaAl(OH)_4$, $NaNO_3$, and $NaNO_2$ resulted in the fit shown in Table II and Fig. 3 with the measured water activity. Although previous work had derived parameters for water activity from pure electrolyte solutions, these SCE parameters were simply fit in a least squares sense to the measured water activities for all of these solutions with a correlation coefficient of 0.98.

The advantage of the SCE approach for water activity is that it provides a great deal of flexibility for estimating water activity for such complex mixtures as Hanford tank wastes. With just two adjustable parameters for each of four major species, we find the water activity scatterplot, Fig. 3, with a correlation coefficient of 0.98.

Water activity plays a role in each of aluminum and phosphate solubilities, and so it is important to have a reasonable expression for water activity. Since water activity was measured for all of these boildowns, those measured water activities were used for each solubility prediction. Water activity is also related to the solution free energy by means of the Gibbs-Duhem integration and so provides a check on the solution free energy. The solution free energy is very important for predicting the solubilities of the major species.

Solubility of $NaNO_3$ at 18 C

The predictions shown in Fig. 4 show deviations on the order of 10-15% for AP-105. Other solubility models for $NaNO_3$ in Hanford wastes [10, 11, 12, 19] have few reports of the accuracy of any of these predictions for concentrating actual waste liquids. Figure 4 also shows (as AP5 ISM) predictions for nitrate solubility for the AP-105 boildown that appear much less accurate.

TABLE I. Starting liquid compositions, M.

Species	**AP-101**	**AP-104 /AW-102**	**AP-105**	**AP-107**	**AW-106**
Na^+	4.9	5.3	5.3	4.7	4.4
NO_3^-	2.1	1.2	3.3	1.9	1.8
NO_2^-	0.50	1.2	0.44	0.65	0.71
OH^-	1.3	0.77	0.56	0.58	0.46
$Al(OH)_4^-$	0.20	0.35	0.23	0.16	0.23
$CO_3^=$	0.30	0.58	0.26	0.48	0.39
PO_4^{3-}	0.035	0.048	0.032	0.030	0.035
$SO_4^=$	0.037	0.032	0.054	0.096	0.081
TOC	0.083	0.28	0.076	0.11	0.11
F^-	0.043	0.012	0.0010	0.024	0.019
Cl^-	0.037	0.10	0.040	0.039	0.049
K^+	0.28	0.065	0.030	0.035	0.045

TABLE II. Solvation cluster equilibria parameters by regressing boildown data to Eq. 1, assuming $\gamma_{DH} = 1$ for expediency.

Species	$\mathbf{K_i}$	$\mathbf{n_i}$	$\mathbf{\nu_i}$	**mol fraction calc, f_i**
NaOH	4.25	1.25	2	m_{OH}/m_{Na}
$NaAl(OH)_4$	24.1	3.08	2	m_{Al}/m_{Na}
$NaNO_3$	0.96	1.28	2	$(1- f_{OH} - f_{Al})\ mNO_3/(mNO_3 + mNO_2)$
$NaNO_2$	0.773	10.69	2	$(1- f_{OH} - f_{Al})\ mNO_2/(mNO_3 + mNO_2)$

TABLE III. Free energies of solvation for major species

Electrolyte	$\mathbf{\Delta G_{sol}}$ **kJ/mol**
$NaNO_3$	-6.14
$NaNO_2$	-9.47
$NaNO_3 \cdot NaNO_2$	-15.6*
$NaAl(OH)_4$	-85**
NaOH	-39.6
$Na_2CO_3.H_2O$	-4.93
$Na_2SO_4.NaF$	-11.2
$Na_3PO_4(NaF.19H_2O)_{0.5}$	-9.02
NaCl	-9.07

**Ternary represents sum of binaries. **Estimated by regression to data.*

Figure 3. Water activity scatterplot, SCE versus measured.

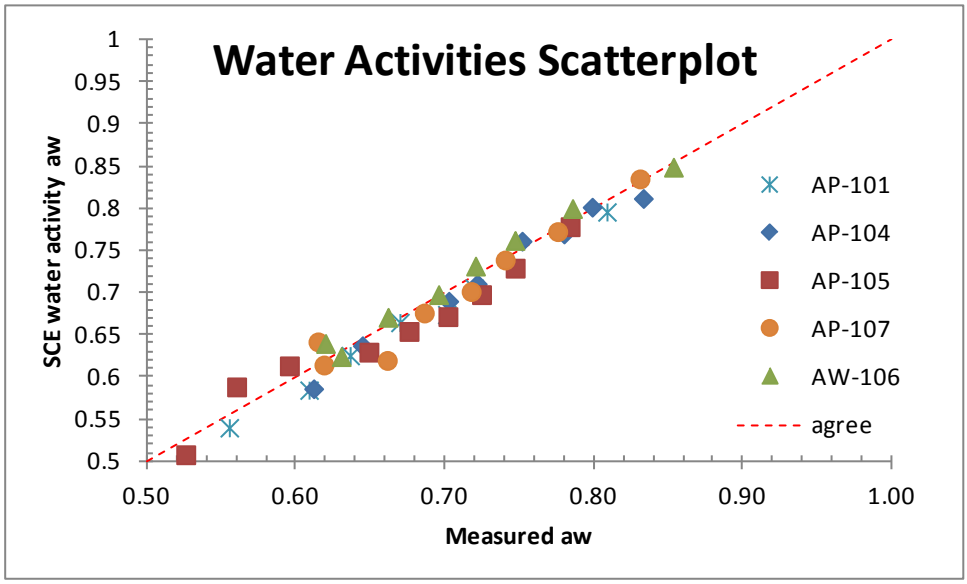

Water activities calculated with the SCE parameters in Table II fit to the measured water activities of the five boildowns shown with a coefficient of 0.98.

Figure 4. Predicted versus measured $NaNO_3$ solubility at 18°C.

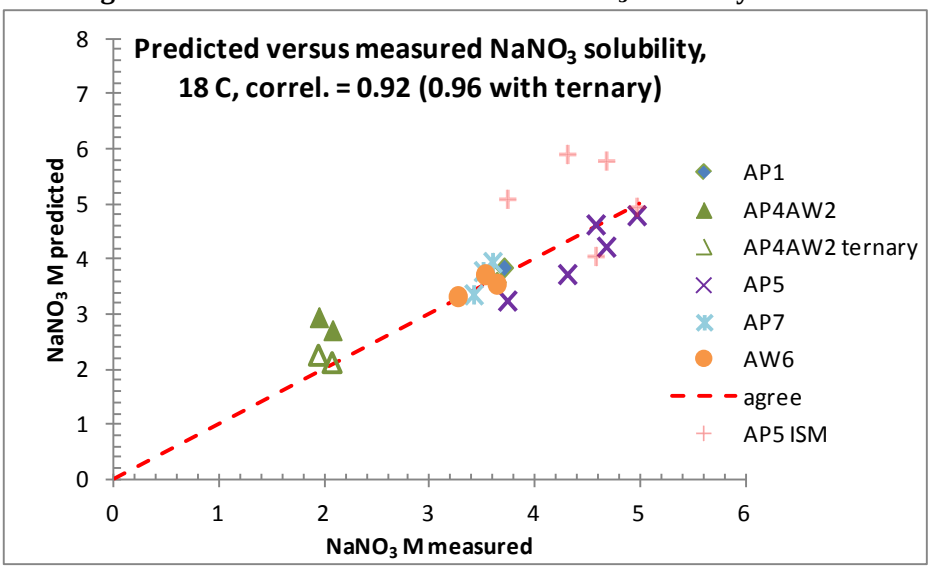

Predictions versus measured $NaNO_3$ solubility at 18°C for all solutions of the boildowns. The precipitation for AP4 occurred at the ternary point as $NaNO_3 \cdot NaNO_2$ and so reflected the sum of $\Delta G_{solNaNO3} + \Delta G_{solNaNO2}$ instead of just $\Delta G_{solNaNO3}$ as noted in text.

Solubility of $NaNO_2$

When more than one species precipitates at the same time, the relative amounts of precipitated species depend on both equilibrium solubility and the kinetics of crystal growth. In such ternary or multinary precipitations, the solution free energy changes with one precipitate can either enhance or suppress the precipitation of another solid in a process known as salting out or salting in, respectively.

Such salting effects due to coprecipitation kinetics can be quite complex and highly dependent on the evaporation rate [14] as well as on nucleation and crystal growth kinetics. For example, the carbonate/sulfate double salt burkeite, $Na_2CO_3[Na_2SO_4]_2$ has been extensively studied in simulated waste evaporates [14] with very similar compositions to these actual wastes, but burkeite was not observed in any of these actual waste boildowns despite the similarity in compositions.

As an example of salting out, nitrite precipitation occurs for AP-105 at a concentration that is well below the nitrite-nitrate triplepoint [15, 16]. This suggests that nitrite precipitation is not at equilibrium but rather is a kinetic precipitate likely associated with nitrate precipitation. For each of the boildowns in Table II, the concentrations of nitrite are equal for one and substantially lower than nitrate for the others. However, the nitrite-nitrate ternary point is reported [15, 16] to be where nitrite is ~1.5 times nitrate concentration as shown in Fig. 5.

Figure 5. Solubilities of nitrate and nitrate (molal) with and without mixing and residual free energies.

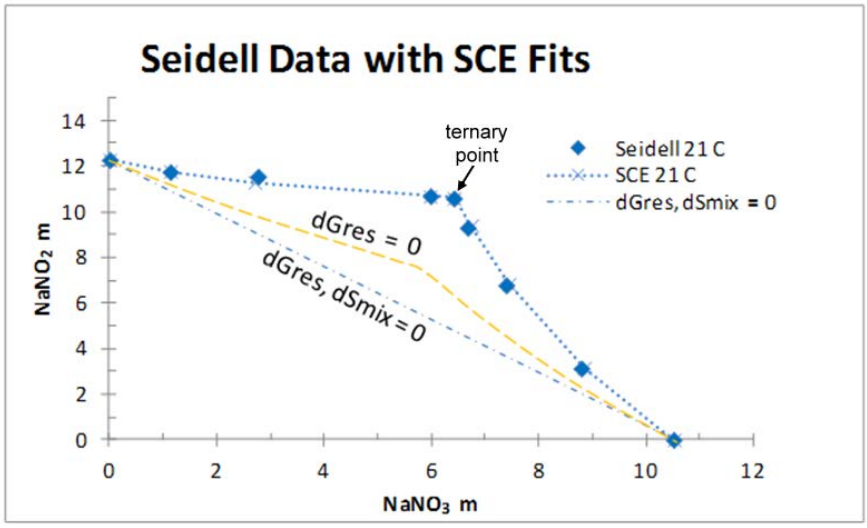

Predictions versus measured $NaNO_3$ and $NaNO_2$ solubilities at 21°C[18]. In principle, the triple point is the only place where $NaNO_3$ and $NaNO_2$ solids coexist. Inclusion of both mixing and residual free energies fits the measured solubilities, but does not allow for the kinetics of precipitation.

The major species begin precipitating $NaNO_3$ followed by $NaNO_2$ and then $Na_2CO_3.H_2O$. The simultaneous presence of two or more solids represents a ternary point, or for more than two solids, a multinary point in the equilibrium phase diagrams. However, previous work shows [9,10] that nitrite should not precipitate from any of these concentrations. The nitrite concentration at the nitrate/nitrite multinery point is ~1.8 times more soluble than nitrate and so solid nitrite should not coexist with solid nitrate for any of these concentrations.

The co-precipitation of $NaNO_2$ with $NaNO_3$ is apparently a kinetic effect most likely due to the dominant precipitation of $NaNO_3$ providing nucleation for $NaNO_2$ as well. Although most pronounced for AP-105, coprecipitation of $NaNO_2$ with $NaNO_3$ occurred to some extent for each of the boildowns. Figure 5 shows the measured solubilities of $NaNO_2$ and $NaNO_3$ along with fits that include no mixing or residual free energy and then mixing only. With both mixing and residual free energies, the model fits the observed trend.

These kind of kinetic effects have been reported for the double salt burkeite, where a kinetic precipitation has been observed in evaporated actual and simulated wastes [14]. Burkeite, though expected, has not been observed in any of the AP tank saltcakes and as well as many other saltcakes [17].

The minor species that precipitate are phosphate-fluoride and sulfate-fluoride double salts as well as oxalate, all solids of which were identified with a combination of PLM, SEM/EDX, and XRD analyses on the solids. The precipitation of these minor species has little effect on the solution free energy and as a result, minor species tend to show simpler dependencies as solubility products [8,9]

CONCLUSIONS

Recent boildowns provide a great deal of data on the compositions of real waste solutions in Hanford tanks as well as on the speciation of precipitates from these solutions upon concentration. These very useful datasets permit the validation of equilibrium solubility models for complex electrolyte mixtures as well as provide kinetic and speciation information that complements equilibrium solubilities.

In the case of $NaNO_3$ solubility, a Gibbs-Duhem integration of the water activity predictions provides a relatively simple thermodynamic prediction for solubility for $NaNO_3$. The predictions are consistent with reported solubility over very wide ranges of compositions and 18 C. Previous work has reported the temperature dependence of these solubilities.

The precipitates for these concentrates are mixtures of the major electrolytes $NaNO_3$, Na_2CO_3, and $NaNO_2$. When two or more electrolytes are in equilibrium with a saturated liquid, this should represent an invariant multinary point in the phase diagram with unique concentrations. However, the kinetics of nucleation and crystal growth along with the presence of multiple soluble species mean that these multinary points will vary, sometimes markedly.

Therefore it is important to calibrate a solubility model for a complex mixture with a set of assays from samples that reflect the kinetics of either precipitation for the case of evaporation or dissolution for the process of washing or leaching. Water activity integrations should have general applicability for solubility predictions for similar liquid compositions in the range of 2-5 M $NaNO_3$ (see Fig. 4) and we look forward to future boildown assays to further validate this approach.

REFERENCES

1. Callaway, W.S., “Results of Boildown Study on Liquid Waste Retrieved from Tank 241-AW-106”, WRPS-1000136, January 2010.
2. Callaway, W.S. “Final Results of Boildown Study on Supernatant Liquid Retrieved from Tank 241-AP-105,” 7S110-WSC-07-143, December 2007.
3. Callaway, W.S., J. S. Page, “Boildown Study on Supernatant Liquid Retrieved form AP-107,” LAB-RPT-12-00008, Rev. 0, January 2013.
4. Callaway, W.S. “Final Results of Boildown on Supernatant Liquid Retrieved from Tank 241-AP-101,” 7S110-WSC-08-145, February 2008.
5. Callaway, W.S. “Final Results of the Boildown Study Supporting 242-A Evaporator Campaign 07-01,” 7S110-WSC-07-110, April 2007.
6. Antoine, C. "Tensions des vapeurs; nouvelle relation entre les tensions et les températures", Comptes Rendus des Séances de l'Académie des Sciences 107: 681–684, 778–780, 836–837, 1888.
7. Agnew, S.F., C.T. Johnston, “Aluminum Solubility in Complex Electrolytes”, Proceedings of Waste Management Conference, Feb. 24-28, Phoenix, AZ, 2013.

8. Agnew, S.F., J.G. Reynolds, C.T. Johnston, “Predicting Water Acitivity for Complex Wastes with Solvation Cluster Equilibria (SCE),” Proceedings of Waste Management Conference, Feb. 26 - Mar. 1, Phoenix, AZ, 2012.
9. Agnew, S.F., R.A. Wilson, W.G. Ramsey, “Solubility Validation from Boildown Data for Hanford Tank Liquids”, Proceedings of Waste Management Conference, Mar. 2-6, Phoenix, AZ, 2014.
10. Belsher, J.D., P.A. Empey, T.M. Hohl, R.A. Kirkbride, F.L. Meinert, J.S. Ritari, K.R. Seniow, E. B. West, “Hanford Tank Waste Operations Simulator (HTWOS) Version 6.6.1 Model Design Document,” RPP-17152, Rev. 6, September 2011.
11. Pierson, K.L. “Evaluation of the HTWOS Integrated Solubility Model Predictions,” RPP-RPT-53089, Rev. 0, 2012.
12. Carter, R., K. Seniow, “Development of a Thermodynamic Model for the Hanford Tank Waste Operations Simulator,” Proceedings of Waste Management Conference, Feb. 26 - Mar. 1, Phoenix, AZ, 2012.
13. Reynolds, J.G., G.A. Cooke, D.L. Herting, R. W. Warrant, “Salt Mineralogy of Hanford High-Level Nuclear Waste Staged for Treatment,” Indus. Eng. Res. 152, 9741-9751, 2013.
14. Walker, D.D., “Stability Tests with Actual Savannah River Site Radioactive Waste,” WSRC-TR-2002-00026, 2002.
15. Addai-Mensay, J., A. Gerson, C.A. Prestidge, I. Ametov, J. Ralston, “Interactions between Gibbsite Crystals in Supersaturated Caustic Aluminate Solutions,” Light Metals, B. Welch, Ed., 159-166, 1998.
16. van Straten, H.A., P.L. de Bruyn, “Precipitation from Supersaturated Aluminate Solutions,” J. Coll. Interface Sci, 102, 260-277, 1984.
17. Nassif, L., “Accelerating Treatment of Radioactive Waste by Evaporative Fractional Crystallization”, Ph.D. Thesis, Georgia Institute of Technology, May 2009.
18. Seidell, A. “Solubilities of Inorganic and Organic Compounds,” D. van Nostrand, New York, NY, 1919
19. Reynolds, D.A., D.L. Herting, “Solubilities of Sodium Nitrate, Sodium Nitrite, and Sodium Aluminate in Simulated Nuclear Waste,” RHO-RE-ST-14P, September 1984.
20. Herting, D.L., G.A. Cooke, R.W. Warrant, “Identification of Solid Phases in Saltcake from Hanford Site Waste Tanks,” HNF-11585, Rev. 0, September 2002.